Alaska Satellite Facility
News & Notes
Winter 2007, volume 4:4

ALOS PALSAR Interferometric Synthetic Aperture Radar (InSAR)

Zhong Lu, U.S. Geological Survey (USGS), Vancouver, WA 98683, phone: (360) 993-8911, email: lu@usgs.gov

The Japan Aerospace Exploration Agency's (JAXA) Advanced Land Observing Satellite (ALOS) was successfully launched on January 24, 2006. ALOS, a follow-on mission for the Japanese Earth Resources Satellite-1 (JERS-1), carries three sensors: 1) the Panchromatic Remote-Sensing Instrument for Stereo Mapping (PRISM) for digital elevation mapping, 2) the Advanced Visible and Near Infrared Radiometer type 2 (AVNIR-2) for land cover characterization, and 3) the Phased Array type L-band Synthetic Aperture Radar (PALSAR) for day-and-night and all-weather observation. ALOS orbits at an altitude of 691.65 km (at the Equator) with a 46-day repeat cycle.

The PALSAR performs in all aspects better than the JERS-1 SAR (Shimada, et al., 2007). PALSAR can operate at four primary modes with diverse polarizations and offnadir angles: (a) high-resolution single-polarization (FBS) mode, (b) high-resolution, dual-polarization (FBD) mode, (c) fully-polarimetric (PLR) mode, and (d) ScanSAR mode (Table 1). The center frequency of PALSAR is 1270 MHz, resulting in a wavelength of 23.62 cm. Because of the distinct difference in radar wavelength (23.62 cm versus 23.53 cm) and imaging geometry, it is generally not feasible to combine ALOS and JERS-1 SAR images to generate a cross-platform interferogram.

The critical baseline for a PALSAR interferogram, in the default FBS mode, can reach 13 km over flat areas (Figure 1). This is due to the larger chirp bandwidth and longer wavelength of L-band, compared to C-band, sensors such as the European Space Agency's (ESA) European Remote Sensing-1/-2 and Envisat, and the Canadian Space Agency's (CSA) RADARSAT-1 (standard beam modes). In addition, PALSAR is yaw-steered, and Doppler centroids of PALSAR images fall within a few hundred hertz of zero Doppler. The orbital tube is controlled within one km or less; therefore, PALSAR images from the same imaging geometry can be combined to produce coherent interferograms. This includes the combination of PALSAR images at different spatial resolutions, between FBS and FBD modes, for interferometric applications. The larger critical baseline for a PALSAR interferogram causes it to be very sensitive to topographic relief. Accordingly, a high-accuracy Digital Elevation Model (DEM) is needed to remove the topographic contribution in the original interferogram in order to generate a deformation map. For a PALSAR interferogram with a large baseline over high topographic relief areas, terrain-induced, localized range offsets need to be considered in order to precisely register two PALSAR images so as to preserve coherence. In essence, the polynomials that measure the offset fields between the PALSAR images should be a function of range, azimuth, and

Continued on Page 2

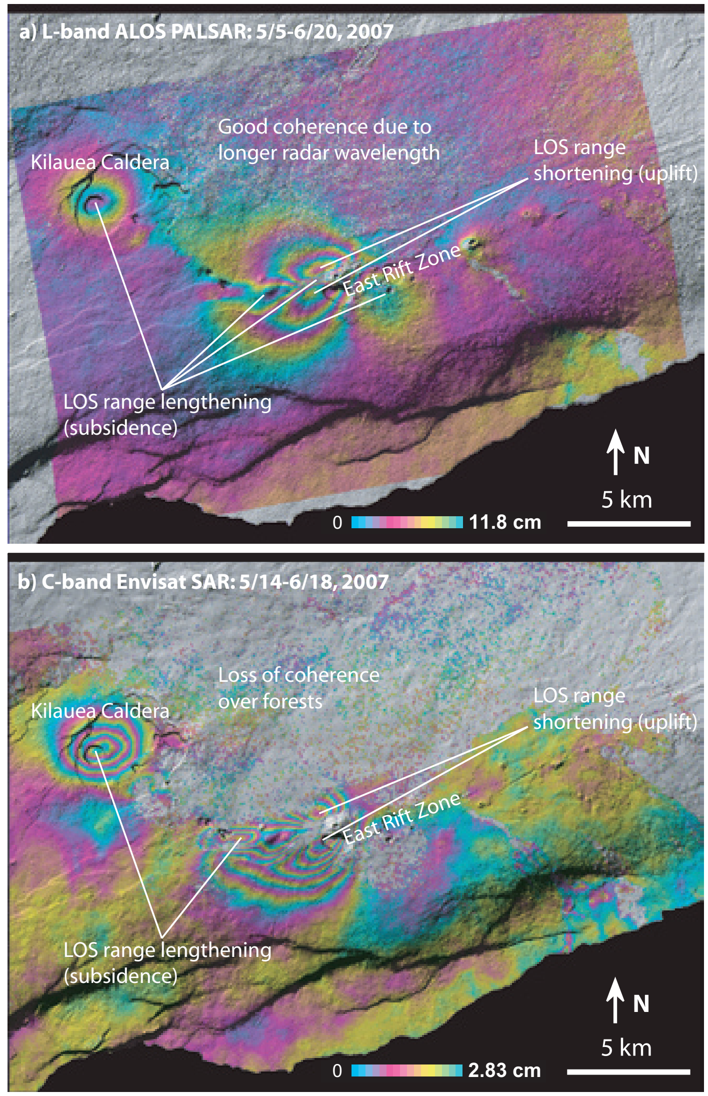

Figures 1a and 1b show two InSAR images that captured the ground surface deformation associated with the June 2007 Father's Day dike intrusion and eruption of Kilauea Volcano, Hawai'i. Figure 1a is a 46-day L-band interferogram from two FBD-mode ALOS PALSAR images acquired on May 5 and June 20, 2007. Figure 1b is a 35-day C-band interferogram from two Envisat SAR images acquired on May 14 and June 18, 2007. Both PALSAR and Envisat SAR images were acquired in ascending passes where the satellites traveled from about S10°E to about N10°W and the SAR sensors were directed ~ N80°E with off-nadir look angles of about 34.3° (PALSAR) and 20.6° (Envisat). The perpendicular baselines are about 320 m and 36 m for the PALSAR and Envisat interferograms, respectively. It is obvious that the L-band interferogram maintained much higher coherence than the C-band one, particularly at the forested areas over the northern part of the island. This is mainly due to the relatively long wavelength of the L-band ALOS PALSAR.

Table 1. PALSAR imaging characteristics at different modes.

Imaging mode	Polarization	Bandwidth (MHz)	Off-nadir angle (°)	SRR (m)	AR (m)	B_{cp} (km)	Swath (km)
FBS	HH* or VV	28	8-60 (34.3*)	4.8	4.5	12.9	40-70
FBD	(HH+HV)* or (VV+VH)	14	8-60 (34.3*)	9.6	4.5	6.5	40-70
PLR	(HH+HV+ VV+VH)*	14	8-30 (21.5*)	9.6	4.5	3.3	20-65
ScanSAR	HH* or VV	14* or 28	18-43 (34.1*)	~50-100	~50-100	NA	250-350

* SRR is the slant range resolution, and AR is the azimuth resolution, and B_{cp} is the critical perpendicular baseline over flat terrain.

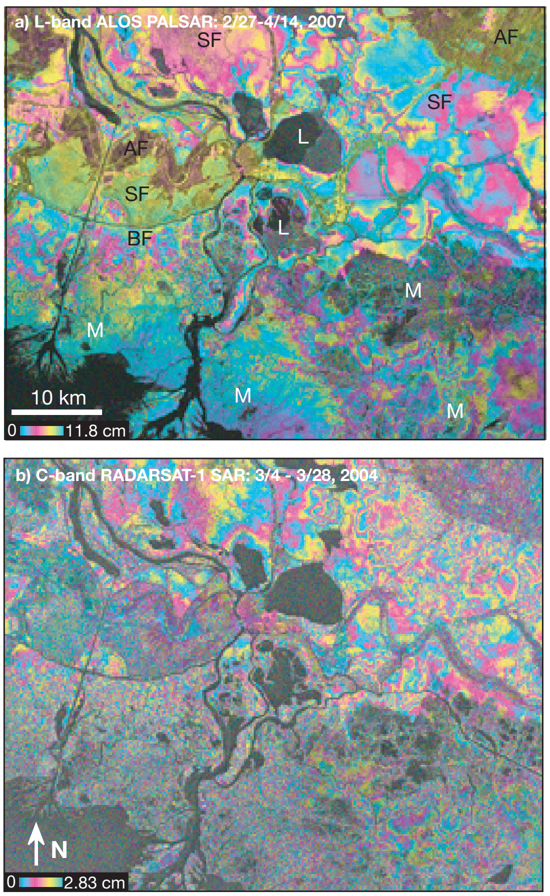

Figures 2a and 2b show two interferograms over coastal wetlands at southeastern Louisiana. Figure 2a is a 46-day L-band PALSAR interferogram acquired from HH-polarized FBS images acquired on February 27 and April 14, 2007, and Figure 2b is a 24-day C-band RADARSAT-1 interferogram acquired from HH-polarized SAR images acquired on March 4 and 28, 2004. Again, it is evident that the 46-day L-band interferogram is generally more coherent than the 24-day C-band interferogram, which in turn can maintain relatively higher coherence than VV-polarized C-band ERS/Envisat images (Lu and Kwoun, 2007). Particularly, the L-band PALSAR interferogram can maintain coherence over bottomland forests and marshes where C-band coherence is often lost. Therefore, L-band interferograms can improve land cover characterization and allow monitoring of water-level changes over coastal wetlands.

Continued from front page

elevation. Finally, burst synchronization between repeat-pass PALSAR ScanSAR images has not been optimized, so ScanSAR interferometry with ALOS PALSAR data is not yet feasible. More information on PALSAR interferometry can be obtained from a technical note by Sandwell and Wei (2006).

The next few years will witness more exciting technical and scientific breakthroughs in many aspects of utilization of ALOS L-band PALSAR imagery. First, L-band PALSAR will enable InSAR deformation mapping at global scales where C-band InSAR can be plagued by loss of coherent signal due to vegetation. Second, fully-polarized ALOS PALSAR will allow better characterization of wetland and vegetation structure and ground features. Third, the combination of polarimetric and interferometric analysis (called Pol-InSAR) will offer a new capability for landscape mapping and monitoring. ALOS Pol-InSAR will enable optimization procedures that maximize the interferometric coherence and target decomposition approaches to the separation of radar backscattering returns from the canopy top, from the bulk volume of the vegetation, and from the ground surface. The difference in interferometric phase measurement then leads to the difference in height between the physical scatterers that possess these mechanisms. Accordingly, ALOS Pol-InSAR imagery will enable significant advances in many fields of application including: a) land cover mapping and wetland mapping, (Figure 2) particularly over regions where weather conditions hinder optical remote sensing, b) inferring soil moisture with a horizontal resolution (several meters) that is not attainable otherwise, and c) mapping forest height and biomass with the generation of "bare-earth" DEMs, and much more. Along with other SAR and optical imagery, ALOS PALSAR will address and provide solutions to many scientific questions related to natural hazard monitoring and natural resource management.

Acknowledgments

ALOS, Envisat, and RADARSAT-1 SAR images are copyrighted JAXA, ESA, and CSA, respectively, and were provided by the Alaska Satellite Facility (ASF) and ESA. This work was supported by funding from the NASA Earth Surface and Interior Program, the USGS Volcano Hazards Program, and the USGS Land Remote Sensing Program. Technical reviews by O. Kwoun and C. Wicks are greatly appreciated.

References

Lu, Z. and O. Kwoun, Radarsat-1 and ERS Interferometric Analysis Over Southeastern Coastal Louisiana: Implication for Mapping Water-Level Changes Beneath Swamp Forests, IEEE Transactions on Geoscience and Remote Sensing, submitted, 2007.

Sandwell, D. and M. Wei, ALOS Interferometry, http://topex.ucsd.edu/alos/, 2006.

Shimada, M., and others, PALSAR CALVAL Summary and Update 2007, IEEE International Geoscience and Remote Sensing Symposium, Barcelona, Spain, 2007.

Faraday Rotation Effects in ALOS/PALSAR Data

Franz Meyer and Jeremy Nicoll, ASF, University of Alaska Fairbanks, Fairbanks Alaska, USA

Since the second half of 2006, ASF has been receiving, processing, archiving, and distributing data of ALOS PALSAR, a fully-polarized L-band SAR sensor. Among other applications, PALSAR data are used for sea ice and vegetation mapping, ice-motion analysis, volcano monitoring, crustal dynamics, and polarimetric studies. These applications demand high data-quality and signal-calibration standards.

In L-band SAR, the influence of the ionosphere on the radiometric, geometric, and polarimetric image quality is of major concern. Ionospheric effects in L-band strongly exceed those observed in C-band, and are, therefore, more significant in PALSAR images than in data of other spaceborne SARs. One of the most prevalent ionosphere-induced distortions in PALSAR data is Faraday rotation (FR), a rotation of the polarization vector of the radar signal. Rotations exceeding 45 degrees are likely to happen during the lifetime of PALSAR, which will significantly reduce the accuracy of geophysical parameter recovery from SAR, if uncorrected. Therefore, the estimation and correction of Faraday rotation effects is necessary to assure high and consistent data quality.

A model-driven FR prediction method, capable of forecasting the FR angles for every PALSAR image in ASF's PALSAR archive, has been developed. This tool should aid in data selection for researchers wishing to avoid FR effects or for those deliberately targeting these effects. The method uses a physical model and ancillary information to come up with reliable predictions of FR angles for every PALSAR image. The predicted Faraday rotation for every PALSAR granule in the Americas ALOS Data Node (AADN) archive as of January 23, 2007, is shown in Figure 1. The histogram illustrates the expected range of FR for the next few years while solar activity is low.

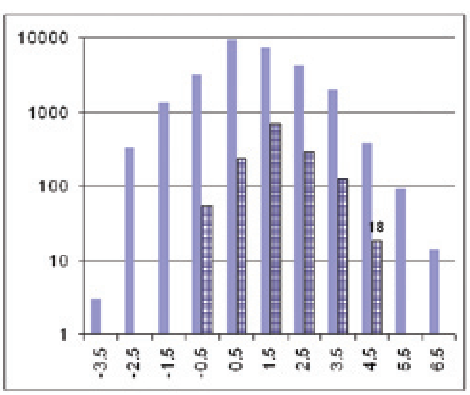

Figure 1. Histogram of predicted FR for ALOS PALSAR holdings through January 23, 2007 at the AADN archive. Y-axis shows number of scenes at each interval on X-axis. Solid bars represent PALSAR data. Hatched bars represent fully polarimetric data only. Note the logarithmic scale.

During the later stages of the PALSAR mission, the solar activity will likely increase and raise the FR angle significantly. The FR prediction tool allows determination of the strength of ionospheric effects in a specific image before ordering. It will be operational on ASF's order interface in the future.

In addition to FR prediction, ASF also supports empirically-derived estimation of FR angles from any full-polarimetric PALSAR data set. The estimator produces two-dimensional FR maps of high accuracy and spatial resolution. The example presented in Figure 2a) illustrates the richness of detail and the utility of the evaluation method. Analysis of an image acquired in the area north of Gakona, Alaska, is shown below. The left panel of Figure 2a displays the SAR image of the analyzed area, while the center panel shows the FR map as a grayscale image. The right panel is reserved for statistical information (e.g., histogram, as well as range and azimuth trends), which is meant to assist the user in data analysis.

This example is particularly interesting as it reveals strong changes in the ionospheric activity within a single SAR image. Several streaks of high FR are visible, which are oriented mainly in east-west directions. This disturbance is most likely caused by auroral activities during the time of the SAR acquisition. Figure 2b shows the along track profile of FR for this ionospheric event. The profile was derived by processing three consecutive images, where the center image is shown in Figure 2a. Besides being essential for the analysis of SAR data quality, FR maps provide valuable information for ionospheric science and can increase our understanding of ionospheric turbulence.

A second example, shown in Figure 3a, covers an area close to the geomagnetic North Pole. Again, variations in the FR

Continued on back page

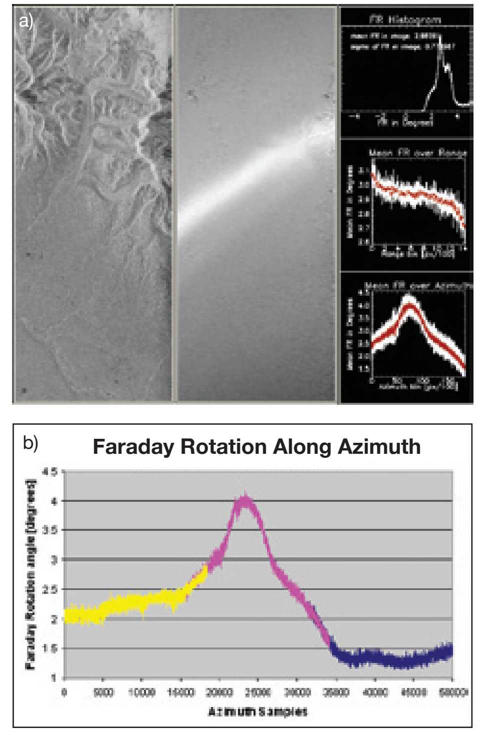

Figures 2a and 2b: a) FR map for an area north of Gakona, Alaska. FR trends in range and azimuth are evident. b) Faraday rotation for three consecutive images with the image in Figure 2a portrayed in the center.

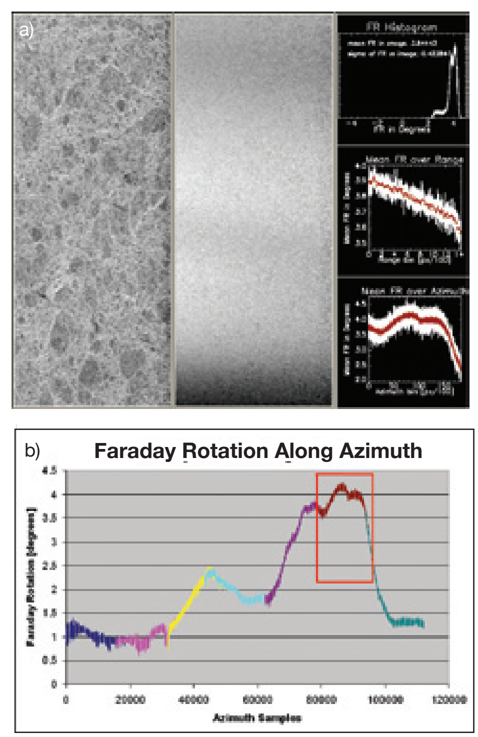

Figures 3a and 3b: a) Example of FR estimation for an area close to the geomagnetic North Pole. FR trends in range and azimuth are evident. b) FR for seven consecutive images. The acquisition of Figure 3a is marked by a red frame.

Continued from page 3

indicate significant turbulence in the ionosphere. The undulations detected in Figure 3a are part of a large-scale disturbance covering an area from -82° to -100° longitude. An along-track profile of the disturbance, mapped from seven consecutive full-polarimetric PALSAR images of the same orbit, is presented in Figure 3b.

As shown in the examples in Figures 2 and 3, FR is present in PALSAR data, reducing data quality. If full-polarimetric data sets are available, FR effects can be compensated. ASF developed a correction algorithm that creates maps of the estimated FR and compensates the image appropriately to restore the original quality of the SAR data. The correction has proven successful for full-polarimetric data sets and can correct for both spatially constant and spatially varying ionospheric effects. Methods for restoring the quality of single- or dual-pol data are not yet available. For these data types, the FR prediction tool will facilitate the search for images with low ionospheric distortions.

Although FR is still a fairly new topic in remote sensing, enormous scientific progress was made during the last few years. FR-prediction methods assist users in selecting data sets suitable for their applications. FR detection and correction algorithms are available for full-polarimetric SAR data and are proven to be effective. Approaches for detecting FR in single and dual-pol data are currently under investigation.

Submissions and Subscriptions

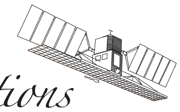

This newsletter, published by the ASF, was created to provide detailed information about special projects and noteworthy developments, as well as science articles highlighting the use of ASF data.

To receive the newsletter by postal mail, please fill out the subscription form linked to the ASF home page at www.asf.alaska.edu. Current and back issues of the newsletter can also be obtained in pdf format through the ASF Web site.

Submissions to the *ASF News & Notes* and suggestions about content are always welcome. If you are interested in contributing materials, please call or send an email to the editor:

Vicky Wolf, ASF User Services
907-474-6166 | uso@asf.alaska.edu

Alaska Satellite Facility
UAF Geophysical Institute
903 Koyukuk Drive
PO Box 757320
Fairbanks, AK 99775-7320